

Effect of particle size distribution on the pre-hydration, hydration kinetics, and mechanical properties of calcium sulfoaluminate cement

Lv, Leyang; Luo, Shitao; Šavija, Branko; Zhang, Hongzhi; Li, Lin; Ueda, Tamon; Xing, Feng

DOI

[10.1016/j.conbuildmat.2023.132497](https://doi.org/10.1016/j.conbuildmat.2023.132497)

Publication date

2023

Document Version

Final published version

Published in

Construction and Building Materials

Citation (APA)

Lv, L., Luo, S., Šavija, B., Zhang, H., Li, L., Ueda, T., & Xing, F. (2023). Effect of particle size distribution on the pre-hydration, hydration kinetics, and mechanical properties of calcium sulfoaluminate cement. *Construction and Building Materials*, 398, Article 132497. <https://doi.org/10.1016/j.conbuildmat.2023.132497>

Important note

To cite this publication, please use the final published version (if applicable).
Please check the document version above.

Copyright

Other than for strictly personal use, it is not permitted to download, forward or distribute the text or part of it, without the consent of the author(s) and/or copyright holder(s), unless the work is under an open content license such as Creative Commons.

Takedown policy

Please contact us and provide details if you believe this document breaches copyrights.
We will remove access to the work immediately and investigate your claim.

Green Open Access added to TU Delft Institutional Repository

'You share, we take care!' - Taverne project

<https://www.openaccess.nl/en/you-share-we-take-care>

Otherwise as indicated in the copyright section: the publisher is the copyright holder of this work and the author uses the Dutch legislation to make this work public.



Effect of particle size distribution on the pre-hydration, hydration kinetics, and mechanical properties of calcium sulfoaluminate cement

Leyang Lv^a, Shitao Luo^a, Branko Šavija^b, Hongzhi Zhang^{c,*}, Lin Li^d, Tamon Ueda^a, Feng Xing^{a,*}

^a Shenzhen Key Laboratory for Low-carbon Construction Material and Technology, College of Civil and Transportation Engineering, Shenzhen University, Shenzhen 518060, China

^b Microlab, Faculty of Civil Engineering and Geosciences, Delft University of Technology, Stevinweg 1, 2628 CN Delft, the Netherlands

^c School of Qilu Transportation, Shandong University, Jinan 250000, China

^d Saint-Gobain Research (Shanghai) Co. Ltd., Shanghai 200245, China

ARTICLE INFO

Keywords:

Calcium sulfoaluminate cement
Particle size distribution
Pre-hydration

ABSTRACT

The particle size distribution (PSD) has a significant influence on the fresh and final properties of cement and its derived products. In this paper, CSA cements with three different mean diameters (D_{50}), ranging from 6.04 to 26.62 μm were prepared by milling. The pre-hydration behavior was quantitatively analyzed, including the degree of pre-hydration, the dynamic change of mineral assemblage and the morphology of the prepared CSA cement exposed to 57%, 75% and 97% relative humidities (RHs) for up to 90 days. Hydration kinetics, porosity, and compressive strength of the cement paste made with fresh and pre-hydrated CSA cement with different PSD were also characterized. The results show that pre-hydration of CSA cement at RH higher than 75% has detrimental effects on the hydraulic activity and strength gain of CSA cement. However, coarser CSA cement ($D_{50} = 26.62 \mu\text{m}$) does not only show better resistance to pre-hydration, but also higher compressive strength and lower porosity.

1. Introduction

Driven by the rising demands for housing and infrastructure, cement consumption increased dramatically in the past decades. Particularly in developing countries like China, cement production has increased more than 4-fold since 1990. An inevitable problem caused by cement production is the vast amount of CO_2 emission which is believed to be responsible for 8% of global anthropogenic CO_2 [1]. To bring the cement sector in line with the Paris Agreement on climate change, its annual emissions must decrease by at least 16% by 2030 [2]. Therefore, both the academia and the industry are looking for reliable alternatives to reduce the environmental footprint of the cement industry.

Among others, calcium sulfoaluminate (CSA) cement has lower CO_2 emission due to the reduced limestone content in the raw materials, lower sintering temperature [3], and lower hardness of sintered clinker [4]. Production of ye'elite, the main phase in CSA cement, releases only one-third of CO_2 released during production of alite, the dominant phase of ordinary Portland cement (OPC) [5]. In addition, compared with OPC, CSA cement has advantages including rapid hardening, high

early strength, low shrinkage and good resistance to harmful ions, e.g. chloride and sulfate ions, among others [6–9]. Consequently, CSA cement can be used for some applications where use of OPC would not be optimal, such as self-levelling floors, structures in the marine environments, filling grouts, and repairs. In addition, it has been shown recently that the hardened CSA cement paste can also be used as a latent heat storage material for seasonal energy storage [10–12]. The heat storage ability is based on the reversible process of hydration/dehydration of ettringite (Aft, $3\text{CaO}\cdot\text{Al}_2\text{O}_3\cdot 3\text{CaSO}_4\cdot 32\text{H}_2\text{O}$), the main hydration product of CSA cement.

Although CSA cement has some excellent properties, properties of hydrated CSA cement are not stable over time. Apart from problems with quality control of CSA cement during the production process, pre-hydration of cement clinker induced by unintentional exposure of cement powder to moisture during the process of cement production, transportation and storage is also a big concern. Previous studies showed that the exposure of cement to a humid environment will result in the pre-hydration of cement powder [13,14]. Silica-based clinker minerals, such as tricalcium silicate (C_3S) and dicalcium silicate (C_2S), begin to

* Corresponding authors.

E-mail addresses: hzzhang@sdu.edu.cn (H. Zhang), xingf@szu.edu.cn (F. Xing).

<https://doi.org/10.1016/j.conbuildmat.2023.132497>

Received 2 March 2023; Received in revised form 10 July 2023; Accepted 11 July 2023

Available online 17 July 2023

0950-0618/© 2023 Elsevier Ltd. All rights reserved.

pre-hydrate at ambient humidity above 85% [15]. Compared to silica-based clinker minerals, aluminate-based clinker minerals such as ye'elimite and tricalcium aluminate (C_3A) are more susceptible to moisture. C_3A was found to hydrate at ambient humidity of 60% RH [15]. This phenomenon has only recently been investigated for CSA cements [16,17]. It was found that the main constituent of CSA cement, ye'elimite, tends to pre-hydrate when exposed to 60% RH. Pre-hydration of cement will decrease the hydraulic reactivity of cement powder, extend the setting time, and reduce its final strength. It is therefore of crucial to minimize the negative effect of pre-hydration on CSA cement.

Particle size distribution (PSD) of cement determines the overall surface area of cement powder that could encounter water molecules (including liquid and gas states) and the distance between individual cement particles. Therefore, PSD is one of the most important factors that influence the fresh and hardened properties of concrete [18–21]. Bentz et al. [18] investigated the impact of PSD on various properties of OPC. They reported that, in lower water-to-cement ratio systems, the use of coarser cement may offer equivalent or superior performance and reduce production costs. As the hydraulic activity of CSA cement is much higher than OPC, the PSD is expected to have a more profound impact on the overall performance of CSA cement. However, to the best knowledge of the authors, this has not been investigated to date. The effect of clinker fineness on the pre-hydration of sulfoaluminate cement is not known, and the influence of sulfoaluminate cement pre-hydration on the hydration process, mechanical properties, and durability are still being explored.

This work aims to study the effect of PSD of cement clinker on the pre-hydration, hydration kinetics, and mechanical properties of CSA cement. This should allow building a relationship between the PSD and the aging (pre-hydration) behavior of CSA cement at various RH before its use in concrete, as well as afterwards (hydration kinetics and compressive strength). To this end, fresh CSA cement powder with three different PSD was produced by grinding the raw CSA clinker particles. The freshly ground cement powder, with the addition of anhydrite, was then exposed to three different ambient humidities (57 %RH, 75 %RH and 97 %RH), for a maximum of 90 days. A series of tests were conducted to characterize the pre-hydration rate, hydration kinetics, and the hardened properties of CSA cement with different PSD. Thermogravimetric analysis (TGA) and X-ray diffraction (XRD) coupled with Rietveld refinement method was applied to quantitatively analyse the dynamic mineral change throughout the pre-hydration and hydration stage. The hydration kinetics of pre-hydrated ye'elimite was monitored using isothermal calorimetry. The morphology and the microstructure of mineral grains were observed using scanning electron microscope (SEM). Low field nuclear magnetic resonance (LF-NMR) was used to measure the porosity of hardened CSA cement. Compressive strength has also been measured on fresh and pre-hydrated CSA cement paste with different PSD. Current research may contribute not only to understanding the effects of PSD on the pre-hydration and hydration behavior of CSA cement but may also provide guidance to the cement industry for improving the performance of CSA cement while reducing the costs from the clinker grind process.

2. Materials and methods

2.1. Materials

Spherical raw CSA clinker, which is used to prepare CSA cement powder with different PSD, was provided by Tangshan Polar Bear Special Cement CO, Ltd. The chemical composition of the milled CSA

Table 1

The chemical composition of CSA clinker was measured by XRF (wt%).

CaO	SiO ₂	Al ₂ O ₃	Fe ₂ O ₃	MgO	TiO ₂	K ₂ O	Na ₂ O	P ₂ O ₅	SO ₃
44.04	10.14	31.7	2.09	2.34	1.21	0.377	0.145	0.139	7.51

cement was measured by X-ray fluorescence (XRF, Thermo Scientific ARL™ PERFORM'X WDXRF, USA), see Table 1. The mineral phase composition of the ground CSA cement determined by quantitative XRD analysis is given in Table 2. Organic solvents, isopropanol and diethyl ether, were used to stop cement hydration, as recommended by RILEM TC-238 SCM [22]. Anhydrite was obtained by burning the calcium sulfate obtained from Aladdin Bio-Chem Technology Co., LTD, at 700 °C for 2 h. Sodium bromide, sodium chloride, and potassium sulphate were used to maintain a constant value of RH in sealed chamber. All chemicals used were analytical grade without further purification.

2.2. Sample preparation

2.2.1. Preparation of CSA clinker powder with different PSD

To obtain fresh CSA clinker powder with different PSD, a planetary ball mill (PM400, Retsch, Germany) was applied to mill the CSA clinker with the following schemes. The coarse cement (CC) was produced by milling the raw clinker for 10 min and then passing the milled clinker through a 150-mesh screen. The medium fineness cement (MC) was produced by milling the raw clinker for 20 min followed by milling the after-sieved clinker for additional 20 min. The fine cement (FC) was obtained by milling the raw clinker for 40 min followed by milling the after-sieved clinker for additional 60 min. As the clinker does not contain gypsum, milled CSA clinker was blended with 26 wt% gypsum to produce a final CSA cement powder with an m value (mol ratio) of 2. The final product was vacuum sealed in a plastic sample bag until use. Laser diffraction particle size analyzer (HELOS-OASIS, SYMPATEC GmbH, Germany) and nitrogen adsorption instrument (3FLEX, Micromeritics, USA) were used to measure the PSD and specific surface area (SSA) of the milled CSA clinker powders, respectively. About 5 g of cement powder was first loaded into the device, and laser diffraction measurements were performed to obtain the PSD ranging from 0.02 to 2000 μm. Values reported herein are averages of five measurements. Prior to measurements, a degassing treatment on the cement powder was carried out under vacuum at 110 °C for 24 h. The specific value of PSD and SSA of the ground CSA clinker powder and anhydrite are shown in Fig. 1 and Table 3, respectively.

2.2.2. Pre-hydration procedure

The pre-hydration process was conducted by exposing the CSA cement powder with three different PSD at 57%, 75% and 97% RH for 7, 28 and 90 days, respectively. The adopted RH values were determined based on our previous study [16]. In this study, it was found that the effects of pre-hydration on CSA clinker were neglectable at low RH, for example, 23% RH and 43% RH. Therefore, exposure condition at low RH values was not included here in this study. The corresponding RHs were maintained in separate sealed glass drying jars using the saturated salt solution method [23]. The ambient temperature, type of saturated salt, label name, and the corresponding standard RH [24] are shown in Table 4. Sodium bromide (NaBr), sodium chloride (NaCl) and potassium sulfate (K_2SO_4) were used to maintain the three different levels of RH. To reach equilibrium, the saturated salt solutions were premixed by heating the solution up to 90 °C followed by cooling down to lab temperature.

Table 2

Mineralogical composition of CSA cement clinker (wt%).

C_4A_3S	β - C_2S	Perovskite	MgO	FeO
60.8	35.3	1.8	1.8	0.2

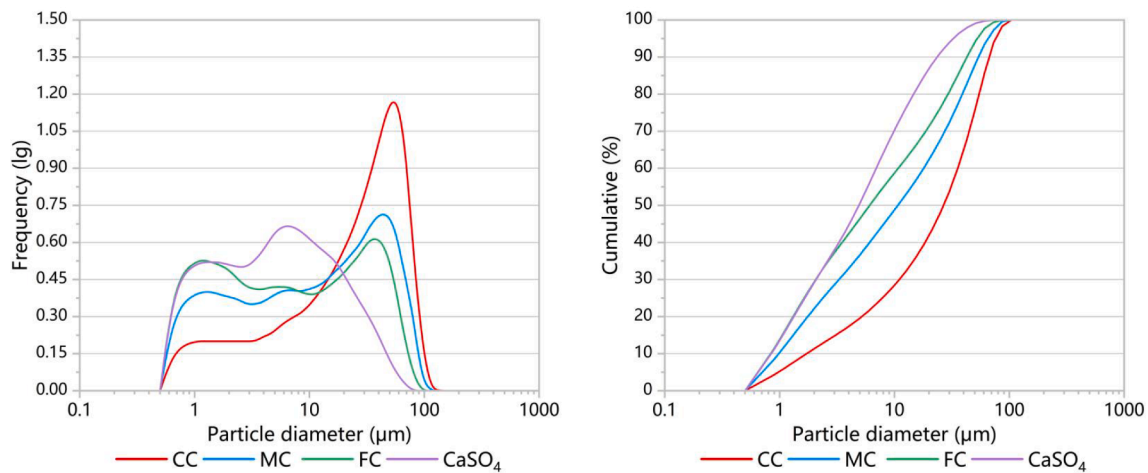


Fig. 1. PSD of the ground CSA clinker powder and anhydrite. CC, MC and FC are stand for coarse cement, medium fineness cement and fine cement, respectively.

Table 3
PSD and SSA of the ground CSA clinker powder and anhydrite.

Sample ID	D10 [μm]	D50 [μm]	D90% [μm]	SSA
CC	1.71	26.62	66.69	0.8607 m ² /g
MC	0.99	10.8	54.31	1.0352 m ² /g
FC	0.85	6.04	43.00	1.2009 m ² /g
CaSO ₄	0.86	4.83	23.14	3.5646 m ² /g

Table 4
Pre-hydration conditions for CSA clinker with different PSD.

Temperature	Saturated salt	Standard RH (%)	Labeled as
25 ± 2 °C	NaBr	57.57%	57
	NaCl	75.29%	75
	K ₂ SO ₄	97.3%	97

Before the exposure of clinker to water vapor, the samples were dried using a silica gel desiccant at the exposure temperature for 1 day. To make sure that the CSA cement powder was sufficiently exposed to the ambient environment, it was evenly spread on glass dishes with a layer thickness of approx. 5 mm. The pre-hydration setup is shown in Fig. 2.

2.2.3. Stoppage of hydration

To investigate the mineral composition of the pre-hydrated CSA cement, solvent exchange method was applied to stop the progress of hydration. To this end, the clinker mineral was immersed in isopropanol and ground in a corundum mill for 15 min. The ground clinker was filtered by vacuum to extract the organic solution. The filtrate was dried in an aerated oven at 40 °C for 10 min and then vacuum sealed in a

plastic sample bag. Since long-term storage of cement could possibly result in instable mineral composition, measurements such as thermogravimetric analysis (TGA), X-ray diffraction (XRD) and scanning electron microscopy (SEM) were performed immediately after the stoppage of hydration.

2.3. Pre-hydration kinetics study

2.3.1. Water sorption kinetics

The kinetics of water sorption was determined by scaling the weight increment ratio (g/g) of pre-hydrated CSA cement exposed to water vapor with respect to the weight of the fresh ground cement powder. To minimize the experimental error, the samples were weighted by an electronic balance immediately as they were taken out from the jar.

2.3.2. Degree of pre-hydration

To calculate the amount of chemically bound water, thermogravimetric analysis (TGA) was carried out on 20 ± 2 mg ground cement samples using a TGA analyzer (STA 8000, PerkinElmer, USA) under flowing nitrogen (40 ml/min). The temperature range for testing was 30–800 °C at a heating rate of 10 °C/min. The chemically bound water, $W_{chem.w.}$, was calculated from the masses at 50 °C ($W_{50°C}$) and 550 °C ($W_{550°C}$), according to [25]:

$$W_{chem.w.} = \frac{W_{50°C} - W_{550°C}}{W_{550°C}} \tag{1}$$

The degree of hydration, α , was calculated as [15,26]:

$$\alpha = \frac{W_{chem.w.}}{W_{max.chem.w.}} - LOI \tag{2}$$



Fig. 2. The setup for cement pre-hydration.

All weights in this formula are relative to the ignited clinker weight: g/g ignited clinker. $w_{max,chem.w.}$ is the mass proportion of chemically bound water of the fully hydrated cement. In this study, the fully hydrated clinker was defined as cement hydrated at 23 °C for 28 days with a water to cement ratio of 1. Therefore, the calculated $w_{max,chem.w.}$ of CSA prepared in this study is 0.56 g. LOI (Loss on Ignition) is the normalized weight loss of the anhydrate cement.

2.3.3. XRD and quantitative phase analysis

To obtain the information on mineral composition, X-ray diffraction (XRD) patterns of the freshly ground and pre-hydrated CSA cement were collected at room temperature (24 ± 2 °C) on X-ray diffractometer (D8 ADVANCE Germany) in a $\theta - 2\theta$ configuration using a Cu K α radiation and equipped with a LYNXEYE detector. The operating voltage and current of the generator were set to 40 kV and 40 mA, respectively. The scan range was $2\theta = 5-65^\circ$ with a step size of 0.02° . The quantitative phase analysis of the CSA clinker was performed using the Rietveld refinement method [27,28]. The overall refinement parameters were the background coefficients, cell parameters, peak shape parameters, phase scales and preferred orientation coefficient, if needed. The quantitative phase content was recalculated to an anhydrous statue by considering the amount of chemically bound water. The structural information of the mineral phases used in the quantitative phase analysis and their corresponding abbreviations are given in Table 5.

2.3.4. Surface morphology

SEM (Gemini SEM 300, Carl Zeiss AG, Germany) was used to observe the surface morphology of CSA cement powder with different PSD exposed to water vapor up to 90 days. To obtain a homogeneous dispersion of cement particles, CSA cement was evenly spread on the conductive tape glued to the sample holder then a rubber aurilave was used to remove the excess powder. Finally, the samples were coated with gold prior to SEM observations.

2.4. Paste study

2.4.1. Hydration heat

The hydration heat of the fresh CSA cement and CSA cement pre-hydrated for 90 days with different PSD was recorded at 20.0 °C using isothermal calorimetry (TAM Air 8-channel, TA Instruments, USA). Before testing, 3 g of CSA cement and 3 g of deionized water was externally mixed in the ampoule for 30 s to make a paste with a w/c of 1. Higher w/c (w/c = 1) was adopted here in order to allow sufficient hydration of the CSA cement [36]. The samples were then placed in the calorimeter and the hydration heat was measured for 72 h. Measurements were normalized by sample weight. In this test, only the sample pre-hydrated in the humidity chamber for 90 days was tested, and the 0-day sample was used as control.

2.4.2. Compressive strength

In order to study the effect of pre-hydration on the mechanical properties of CSA cement with various PSD, cement pastes with a w/c of 0.7 were made using freshly milled CSA cement (0 day) and CSA cement pre-hydrated for 7, 28 and 90 days. After hand mixing the mixture in a plastic bottle for 3 mins, the cement pastes were poured into 20 mm cube

molds. The molds were then covered with plastic film and cured at 23 °C for 24 h before demolding. The cubes were demolded after 24 h of sealed curing and then placed in the moist room (100% RH, 23 °C) for another 27 days. Compressive strength testing was carried out on 20 mm cubes using a mechanical testing device (YAW-300B, Julong, China) at a loading rate of 1200 ± 200 N/s. For each mixture, at least three samples were tested at each age, and the coefficient of variation (COV) was generally less than 15%.

2.4.3. Total porosity

The total porosity of the pre-hydrated CSA cement paste hydrated for 28 days was measured using low-field nuclear magnetic resonance (low field-NMR) (MesoMR12-060H-I, Niumay Analytical Instrument Co., Ltd., China). Samples for low field-NMR were obtained by coring the inner part of the cubic cement paste specimens used for compressive strength testing. To protect them from further hydration and carbonation, they were first rinsed with isopropanol followed by diethyl ether and vacuum dried at 40 °C for 3 h. The vacuum-dried samples were sealed in plastic sample bags until testing. Before the test, the samples were placed in vacuum chamber for 3 h and then immersed in water under vacuum for 1 h. Following that, the samples were kept in the vacuum chamber under water for another 18 h to reach full water saturation. After wrapping the samples with polyethylene film, the water saturated samples were subjected to the low field-NMR using CPMG pulse sequence test protocol [37]. The sampling frequency (SW), the echo time (τ), the repeated sampling delay (TW), the accumulation number (NS) and the number of echoes (NECH) were set to 200 kHz, 100 μ s, 1500 ms, 2000, and 16, respectively.

3. Results and discussion

3.1. Water sorption kinetics

Fig. 3 shows results of the water adsorption test obtained on CSA cement prepared with different PSD and exposed to different RH. The weight increase of the clinker powder was recorded for a maximum of 90 days. At 57 %RH, no significant water adsorption was observed for all CSA cement of various PSD. However, as the exposure RH was increased from 57% to 75%, the weight of CSA cement with different PSD was found to increase linearly with the exposure time for the first 28 days. It is noteworthy that the water adsorption of CC sample (0.017 g/g) showed a lower value than that of MC and FC sample at 28 days (0.027 and 0.023 g/g respectively). This can be attributed to the relatively larger particle size with lower surface area of the course clinker powder (CC), which reduced the hydraulic activity of the CSA cement. With elapsed exposure time, this difference became more obvious. At 90 days, the water adsorption of CC is about 0.1 g/g, while the water adsorption of MC and FC sample increased steadily up to 0.14 and 0.16 g/g, respectively. When the exposure RH was increased from 75% to 97%, higher availability of moisture in the environment led to sharper increase of the overall weight of the clinker powder. The water adsorption rate of CC, MC and FC sample, was found to increase from 0% to 0.20, 0.25 and 0.27 g/g in the first 7 days, and further up to 0.25, 0.30 and 0.32 g/g after 28 days. After that, however, the exposure of CSA cement to 97 %RH for additional 62 days led to only about 0.02 g/g increase of bound water in each sample. The difference in trends of CC, MC and FC samples in Fig. 2c confirms that the water adsorption rate of CSA cement increased with the decrease in particle size of CSA cement powder.

Water adsorbed on the CSA cement powder consists of two parts: evaporable water which is physically adsorbed on the surface of the clinker powder, and the chemically bound water in the hydrates. The pre-hydration of CSA cement powder is directly related to the chemically bound water. To have a better understanding of the progress of pre-hydration at various conditions, the amount of chemically bound water was calculated using Eq. (1), based on the TGA data.

Fig. 4 shows the increase in the amount of hydration water that

Table 5

ICSD collection codes used for XRD-Rietveld quantitative analysis.

Phase name	Formula	ICSD codes	Ref.
Orthorhombic ye'elimite	$C_4A_3S^-$	80,361	[29]
Anhydrite	CS^-	15,876	[30]
β -C2S	$\beta-C_2S$	81,096	[31]
Ettringite	$C_6AS^-_3H_{32}$	155,395	[32]
Monosulfate	$C_4AS^-H_{12}$	100,138	[33]
Perovskite	$CaTiO_3$	158,171	[34]
Periclase	MgO	9,863	[35]

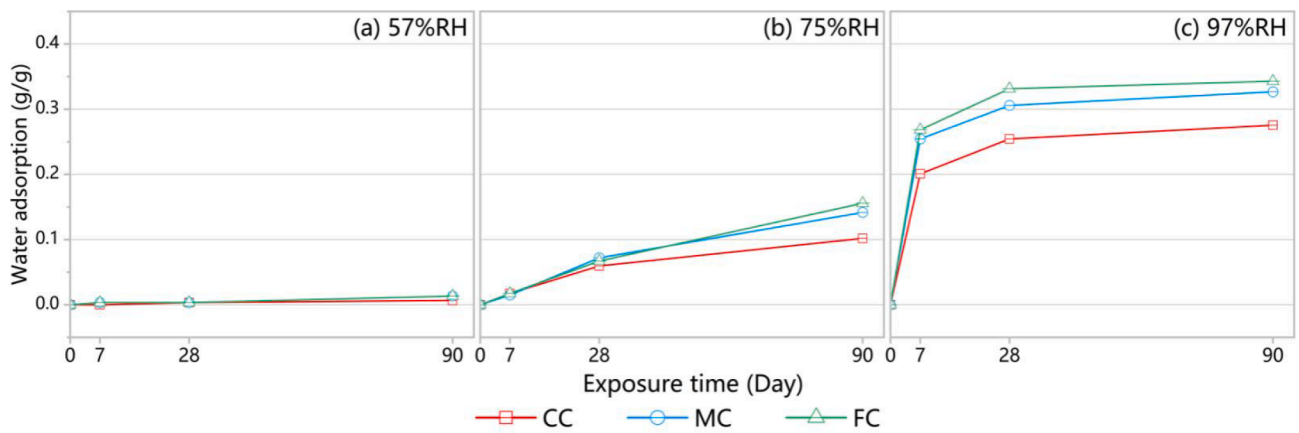


Fig. 3. The water adsorption of CSA cement powder with three fineness and exposed to water vapor of (a) 57%, (b) 75%, (c) 97 %RH for a maximum 90 days.

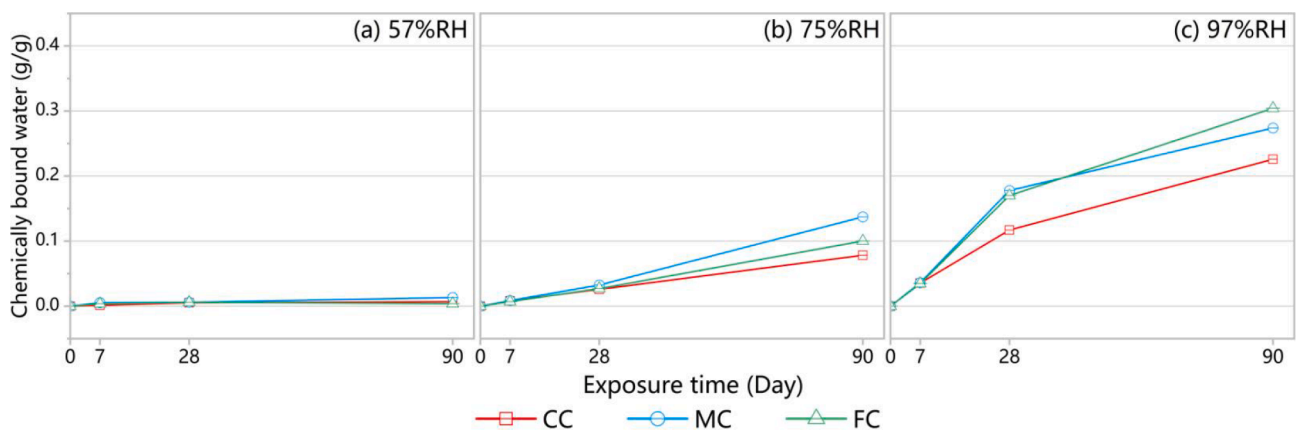


Fig. 4. The amount of chemically bound water held by three fineness of clinker exposed to water vapor of (a) 57 %RH, (b) 75 %RH, (c) 97 %RH for a maximum 90 days.

chemically bound on the cement powder. As can be seen in Fig. 4a, very little chemically bond water was present on the CSA cement sample stored at 57% RH for up to 90 days. For the samples exposed to RH of 75%, the chemically bound water ratios of all three cement powders (FC, MC and CC) increased linearly. Unexpectedly, the MC sample had the highest water absorption rate under this environment, rather than the FC sample with the finer particle size. This may be caused by the higher packing density of FC sample which delayed the progress of pre-hydration. Richartz et al. reported that smaller cement particles result in better packing of cement powder and smaller pore spaces, and thus better resist the ingress of water vapor from the ambient air to the inner part of cement bed [38]. Similarly in this study, due to the relatively finer clinker powder of FC than MC, the higher packing density of FC sample made it harder for the water molecules to penetrate the inner part of the cement bed at 75% RH. As a result, compared with MC, the FC sample showed lower amount of chemically bound water and better resistance to pre-hydration over the 90 days exposure. At 97% RH, this was still the case during the first 28 days, as the amount of chemically bond water of MC sample was slightly higher than that of FC sample. However, with longer exposure time, the densely packed cement powder of FC sample cannot prevent the high concentration of water molecules from penetrating the cement bed further. Under this condition (exposed to 97 %RH for more than 28 days), the amount of chemically bound water in the cement was only related with the PSD of CSA cement powder: the finer the cement is, the higher the amount of chemically bound water. Moreover, only a slight increase of the chemically bond water was measured at 7 days (Fig. 4c), which is different from the results of water absorption tests shown in Fig. 4c which showed significant

weight increases in the first 7 days. This indicates that the weight increase of the CSA cement exposed to 97% RH in the first 7 days is mainly originated from the physisorbed water in the clinker powder rather than the chemically bound water. The CC sample showed the best resistance to pre-hydration.

3.2. Degree of pre-hydration

Based on the TGA results, the pre-hydration degree of CSA cement with different PSD is calculated with Eq. (2), and the results are summarized in Table 6. The values in the table should not be taken as exact figures, but as indicators of the progress of hydration.

As can be seen from the table, the degree of pre-hydration was low

Table 6

Degree of pre-hydration (%) of CSA cement with three PSD that exposed to various relative humidities at 7, 28, and 90 days.

Relative humidity	Sample name	Exposure time (days)			
		0	7	28	90
57%	CC	0	0	1.1	1.8
	MC	0	1.4	1.8	3.4
	FC	0	1	1.8	1
75%	CC	0	2.1	6.6	19.8
	MC	0	2.2	8.2	34.7
	FC	0	1.8	6.8	25.4
97%	CC	0	9.0	29.6	57.2
	MC	0	9.1	45	69.4
	FC	0	8.8	43.1	77

(less than 4%) when the CSA cement clinkers were exposed to 57% RH for up to 90 days. The fluctuation in the results can be attributed to the inevitable exposure of the cement clinker to humid air during the experiment and the carbonation of trace amount of oxide even at low RH [15]. As the ambient RH increased from 57% to 75%, the pre-hydration became more pronounced. The pre-hydration degree of the MC sample is about 34.7% at 90 days, which is significantly higher than that of the CC sample (19.8%) and the FC sample (25.4%). Under 98% RH exposure, the pre-hydration of all three cement powders were more severe. After the exposure of CSA cement to 97% RH for 90 days, finer cement clinker showed to be more sensitive to higher RH: 77% of the hydraulic activity of FC sample was consumed, followed by 69.4% of the MC sample, and 57.2% of the CC sample. Based on the data shown in Table 6, it can be concluded that CSA cement with coarser PSD have better resistance to

the ambient humidity in the air.

3.3. Phase assemblage of pre-hydrated CSA cement

3.3.1. XRD and TG analysis

To further investigate the effect of PSD an exposure condition on the pre-hydration of CSA cement from the perspective of mineralogy, XRD and TGA were used to characterize the dynamic evolution of phase assemblages in the pre-hydrated CSA cement with various PSD. The result was compared with the freshly milled CSA cement powder.

3.3.1.1. 57 %RH. As can be seen from the XRD patterns that (Fig. 5a1, b1 and c1), no obvious change in the mineral composition of the CSA cement powders is characterized throughout the 90 days exposure test,

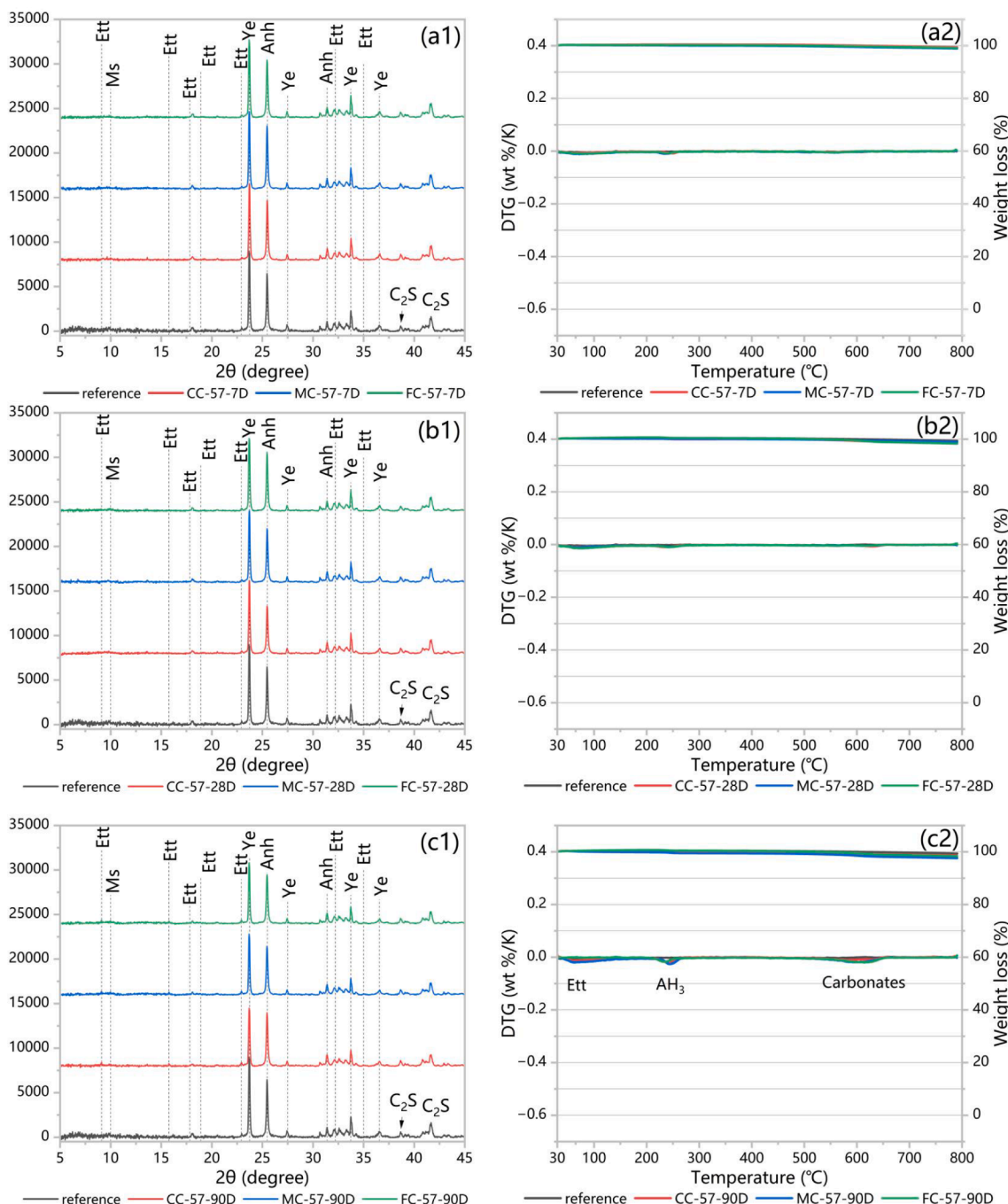


Fig. 5. XRD (a1, b1, c1) and TG (a2, b2, c2) result of CSA cement clinker with different PSD pre-hydrated at 57 %RHfor 90 days.

except for a slight decrease in the intensity of the characteristic peak of ye'elimite (Ye) and anhydrite (Anh) with the prolongation of exposure time from 7 to 90 days. Beta-calcium disilicate (C_2S), ye'elimite (Ye) and anhydrite (Anh) are the main crystalline minerals observed in the CSA cement powders. However, characteristic peaks assigned to the ettringite (overlaps with gypsum), aluminate hydrates and decomposition of carbonation product were observed in the derivative thermogravimetry (DTG, left-axis) at 50–150 °C, 220–300 °C and 550–650 °C, respectively. This is contrast with our previous study, where the phase-pure ye'elimite and ye'elimite mixed with anhydrite were found chemically to be stable at 57% RH within the 180 days [16]. The reason for this is not known. Possible explanations include the unintentional exposure of cement to humid air and the impurity of CSA clinker minerals. Unlike

the phase-pure ye'elimite in our previous study, the CSA clinker applied in this study is a commercial product. The incorporation of foreign oxides in the structure during the cement production may change the hydration properties and thus increase the sensitivity of CSA cement to the water molecules [39]. Moreover, trace amounts of oxides, such as MgO and CaO, can also be included in the CSA cement production. CaO is able to hydrate even at very low RH and to be carbonated with the present of humid air and CO_2 [40].

3.3.1.2. 75 %RH. As the RH is increased to 75%, no significant change in the mineral composition was observed from the XRD pattern in the first 7 days (Fig. 6a1). Meanwhile, only slight weight loss could be detected at 50–150 °C and 230–300 °C by the DTG (Fig. 6a2). With the

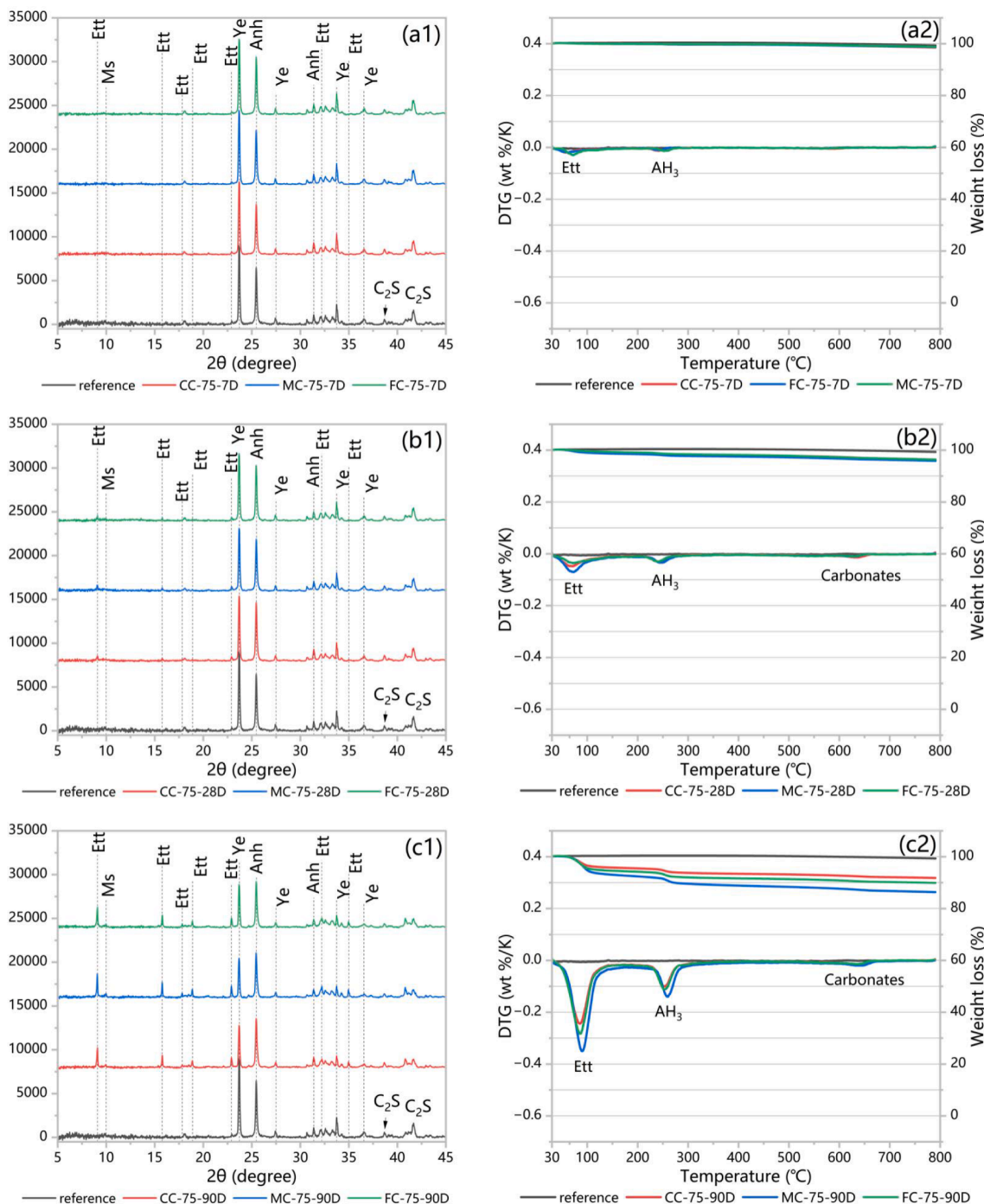


Fig. 6. XRD (a1, b1, c1) and TG (a2, b2, c2) result of CSA cement clinker with different PSD pre-hydrated at 75 %RH for 90 days.

extension of exposure time from 7 to 28 days, the intensity of characteristic peak of ettringite could be observed in the XRD pattern, accompanied with the decreased peak intensity of ye'elimite (Fig. 6a2). This is further supported by the DTG curves, where two distinct weight loss peaks associated with the dehydration of ettringite (50–150 °C) and aluminate hydrates (220–300 °C) are present [5]. After 90 days of exposure, this trend became more significant as more ettringite and aluminate hydrates are formed. Due to their lower specific surface area, CC samples showed the lowest total weight loss, followed by the FC and MC samples. The packing density theory, described in section 3.1, can explain why more hydration products were observed in the MC rather than the FC sample.

3.3.1.3. 97 %RH. The pre-hydration of all three samples was more pronounced at elevated RH of 97%, as shown in Fig. 7. More ettringite and aluminate hydrates could be formed in highly humid air after 90 days of exposure. CC samples showed the highest resistance to high RH environment. In addition, as can be observed in the XRD pattern (Fig. 7 b1 and c1) and DTG curves (Fig. 7 b2 and c2), with the prolongation of exposure time the characteristic peak of ettringite in the FC sample is higher than that of the MC sample, a trend different from that observed in 75% RH. This suggests that the significant higher water activity at 97 %RH decreased the effect of packing density effect of fine particle in the FC sample, which enabled the penetration of water molecules into the cement bed. As a result, the pre-hydration was linearly correlated with the PSD of CSA cement powder. This further confirms that coarser

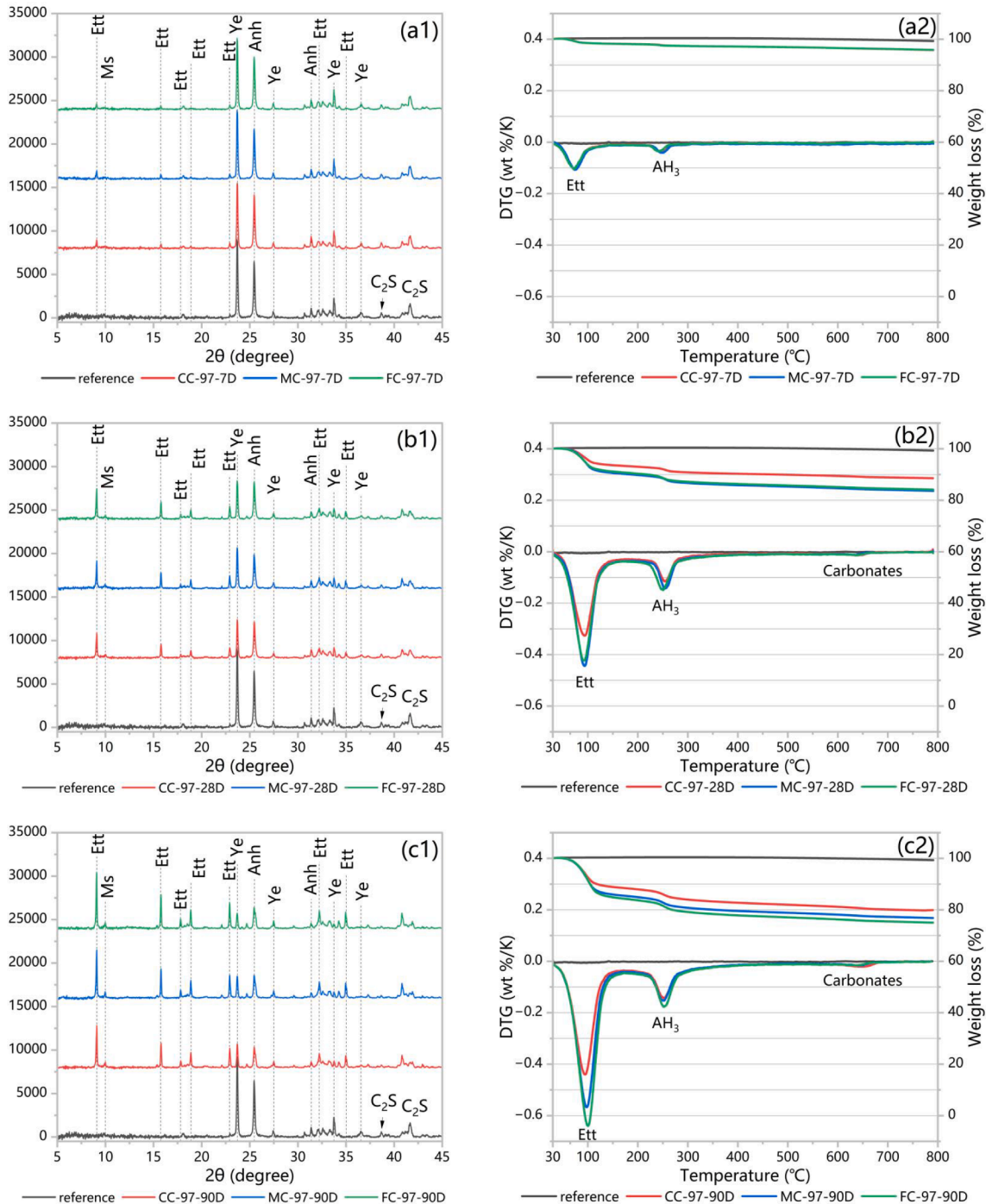


Fig. 7. XRD (a1, b1, c1) and TG (a2, b2, c2) result of CSA cement clinker with different PSD prehydrated at 97%RH for 90 days.

CSA cement with lower SSA is less affected by the highly humid environment.

3.3.2. QXRD analysis of phase assemblage

To further illustrate the dynamic change in mineral composition of the CSA clinkers with different PSD that pre-hydrated at 57%, 75% and 97% RH, Rietveld refinement was used to calculate the phase assemblage of the pre-hydrated clinker powder at 0, 7, 28 and 90 days. As can be seen from the (Fig. 8a, b and c), no obvious changes in crystalline mineral composition were observed for all three sized CSA cement at 57% RH except trace amount of ettringite. In addition, the proportion of minor phases such as Perovskite and MgO remained stable over the 90 days. As the ambient humidity increased to 75% RH, ettringite and XRD amorphous phase (mainly alumina hydrates) formed as the main pre-hydration product in the CSA cement with the depletion of ye'elimite and anhydrite (Fig. 8d, e and f). However, in contrast with the pre-hydration behavior of ye'elimite, the content of C₂S remained almost constant throughout the 90 days at 75% RH. Previous studies demonstrated that C₂S starts to hydrate only at 95% RH after 1 year of water

vapor exposure at 20 °C [15]. When the exposure RH increased to 97% RH, more ettringite was formed with the extension of exposure time. Small amount of monosulfate were detected at 7 and 28 days, and disappeared at 90 days. It is known that the monosulfate will form under the condition that less calcium sulfate was provided during the hydration process [41]. This can be attributed to the lower dissolution rate of anhydrite at the early age of pre-hydration, resulting in insufficient supply of sulfate in the pre-hydration process. With the increasing of anhydrite dissolution rate, the existing monosulfate gradually converted to ettringite. In addition, it was found that, after 90 days of exposure at 97% RH, the phase content of C₂S in CC, MC and FC samples decreased by 12.8%, 11.11% and 8.5%, respectively. This suggests that the C₂S began to react in highly humid air. Although the pre-hydration product of C₂S cannot be characterized by XRD, it is expected that the pre-hydration product of C₂S is amorphous C-S-H gel, which has been included in the portion of XRD amorphous phase.

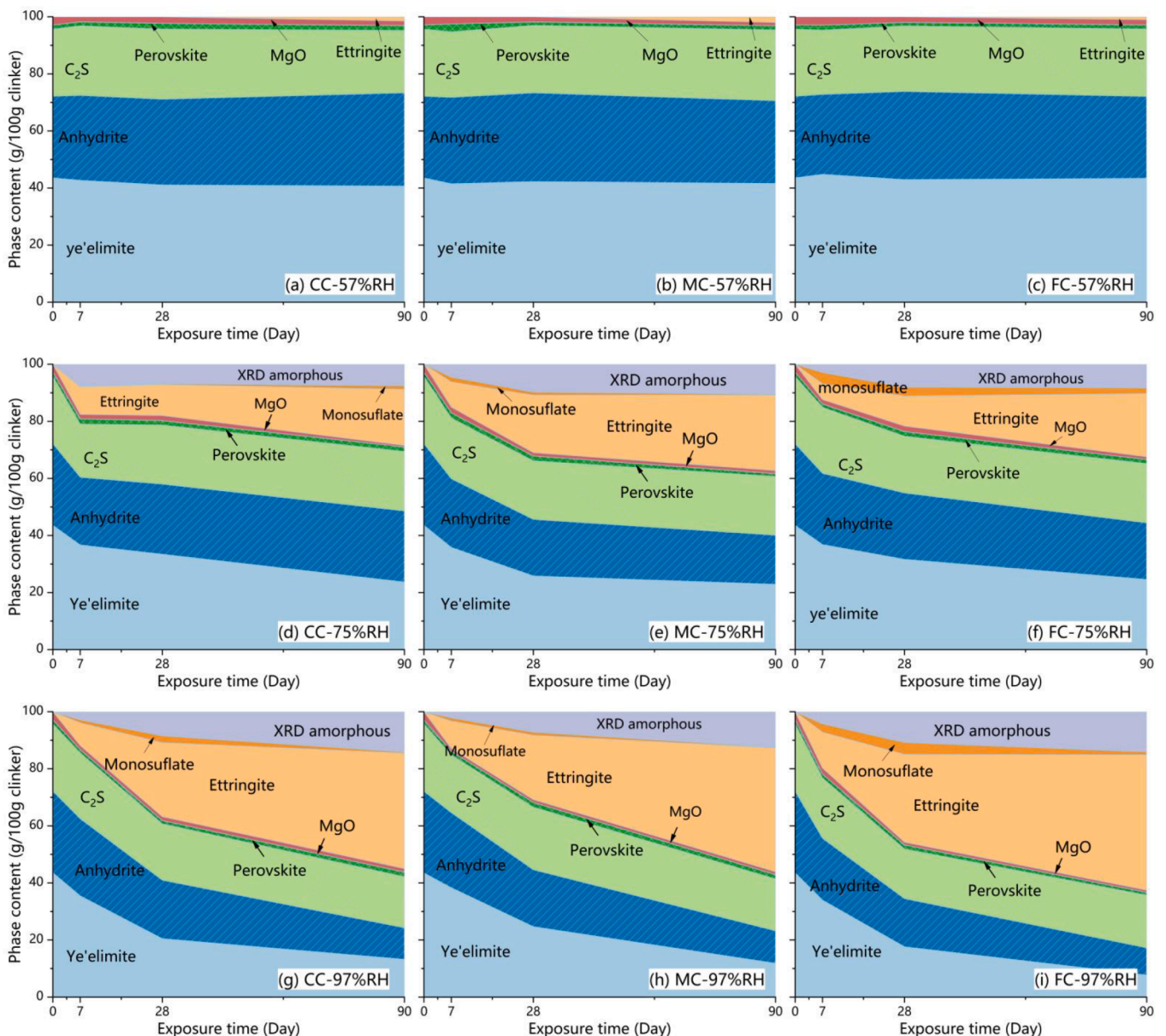


Fig. 8. Evolution of phases assemblage of CSA cement with different PSD that pre-hydrated at 57% (a, b, c), 75% (d, e, f) and 97% RH (g, h, i) for up to 90 days.

3.4. Surface morphology

SEM was used to observe the changes in morphology of CSA cement before and after exposure to different RH. As no significant differences of the morphology were found among the FC, the MC and the CC sample, only the SEM images of anhydrous cement and CC sample exposed to 57%, 75% and 97% RH for 90 days are reported here (Fig. 9). The morphology of the CSA cement stored under 57% RH for 90 days (Fig. 9b) is similar to that of unhydrated cement (Fig. 9a). It seems that no hydration products have formed on the surface of clinker. In 75% RH, needle-like hydration products formed on the surface of cement grains. This is in consistent with the results of XRD and TG, where ettringite and monosulfate was found as main pre-hydration products in the cement clinker with the consumption of ye'elite and anhydrite. As the ambient RH further increased from 75% to 97%, column-like hydration products were observed. The higher RH not only promoted the formation of ettringite, but also affected the texture and the morphology of the hydrated cement clinker. The changes in morphology of hydration products can be attributed to the improved dissolution of anhydrite at 97% RH that promote the transformation from needle-like ettringite and monosulfate to column-like ettringite.

3.5. Cement paste study

3.5.1. Compressive strength and porosity

Fig. 10 shows the compressive strength and the corresponding porosity of cement paste made from fresh CSA cement (0 day) and CSA cement after it was pre-hydrated at different RH for 7, 28 and 90 days. As can be seen, the physical properties of CSA cement paste, including compressive strength and porosity, were not affected by the exposure of cement to 57% RH for up to 90 days. The compressive strength (Fig. 10a1) and the porosity (Fig. 10a2) of both CC-57, MC-57 and FC-57 specimens remained almost unchanged. Compared to the MC and the FC samples, the CC samples showed the highest compressive strength and the lowest porosity. Moreover, it was noticed that a relatively large deviation of the compressive strength value was characterized in the

test. The large scatter was believed to originate from the small sample size (20 mm cubic meter) due to the amount of pre-hydrated CSA cement was insufficient to make standard specimens.

With the increase of ambient RH from 57% to 75%, it is interesting to note that the compressive strength of the CC-75-7 and MC-75-7 specimens, made from CSA cement exposed to 75% RH for 7 days, increased by 5% and 12%, respectively (Fig. 10b1). The reduced porosity (Fig. 10b2) shows that exposing CSA cement to 75% RH less than 7 days will not lead to the degradation of CSA cement, but could even enhance its final properties. This can be explained by the passivation layer theory [16], in which an induction period was observed when ye'elite was exposed to a humid environment. The induction period delayed the progress of pre-hydration of CSA cement at an early age, allowing a stable hydraulic activity of the cement to have remained.

Similar results can also be observed in Fig. 10c1 where the compressive strength of the cement paste remained stable, even when CSA cement was exposed to 97% RH for 7 days. Nevertheless, for CSA cement exposed to 75% and 97% RH, the compressive strength shows a decreasing tendency as the exposure time extends from 7 to 90 days. The compressive strength is not measurable on CSA cement exposed to 97% for 90 days as no cementing was present anymore. Moreover, it was noticed that, even though the porosity at 90 days under 75% RH is similar to that at 28 days under 97% RH, the strength of the latter is much smaller than the former. It demonstrates that the porosity itself cannot be regarded as the single indicator of the strength, even for the same type of cement, as the hydraulic activity of the cement may differ considerably.

3.5.2. Hydration heat

Fig. 11 shows the heat flow and accumulated heat of fresh CSA cement powder (0 day) and CSA cement powder with different PSD pre-hydrated at 57%, 75% and 97% RH for 90 days. Considering the effect of environmental disturbance, the stability of the instrument and the inhomogeneity of sample, the confidence interval for the measurement is defined as 95%.

According to the measured cumulative heat, it was found that,

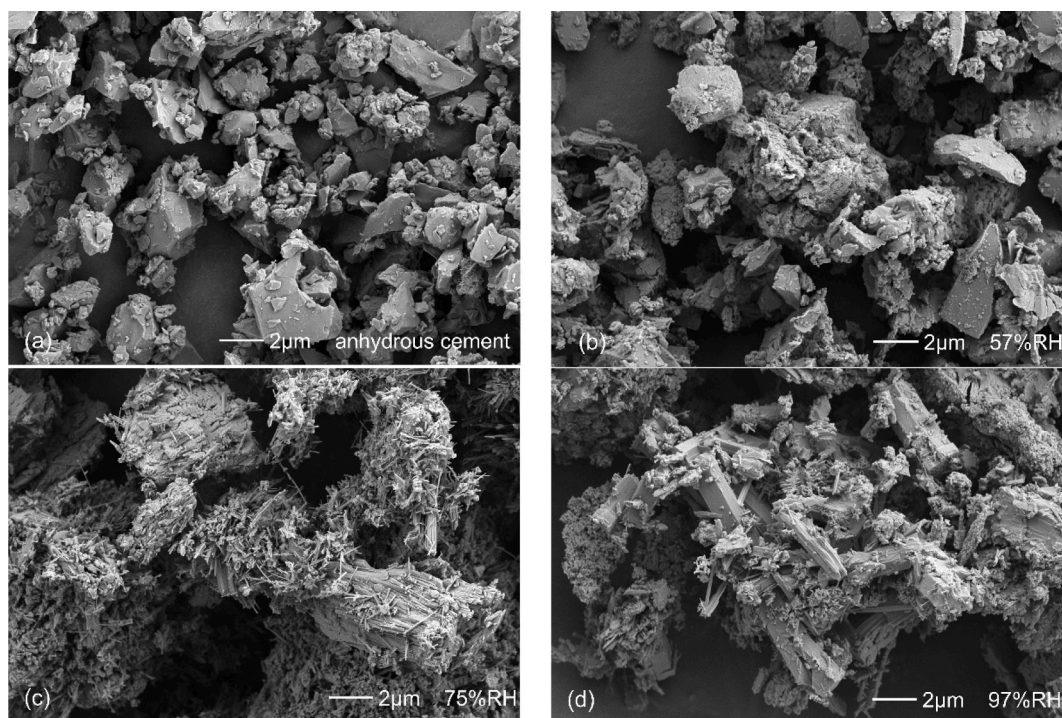


Fig. 9. Surface morphology of anhydrous CSA cement clinker grains (a) and CSA cement clinker grains pre-hydrated at 57% RH (b) 75% RH (c) 97% RH (d) for 90 days.

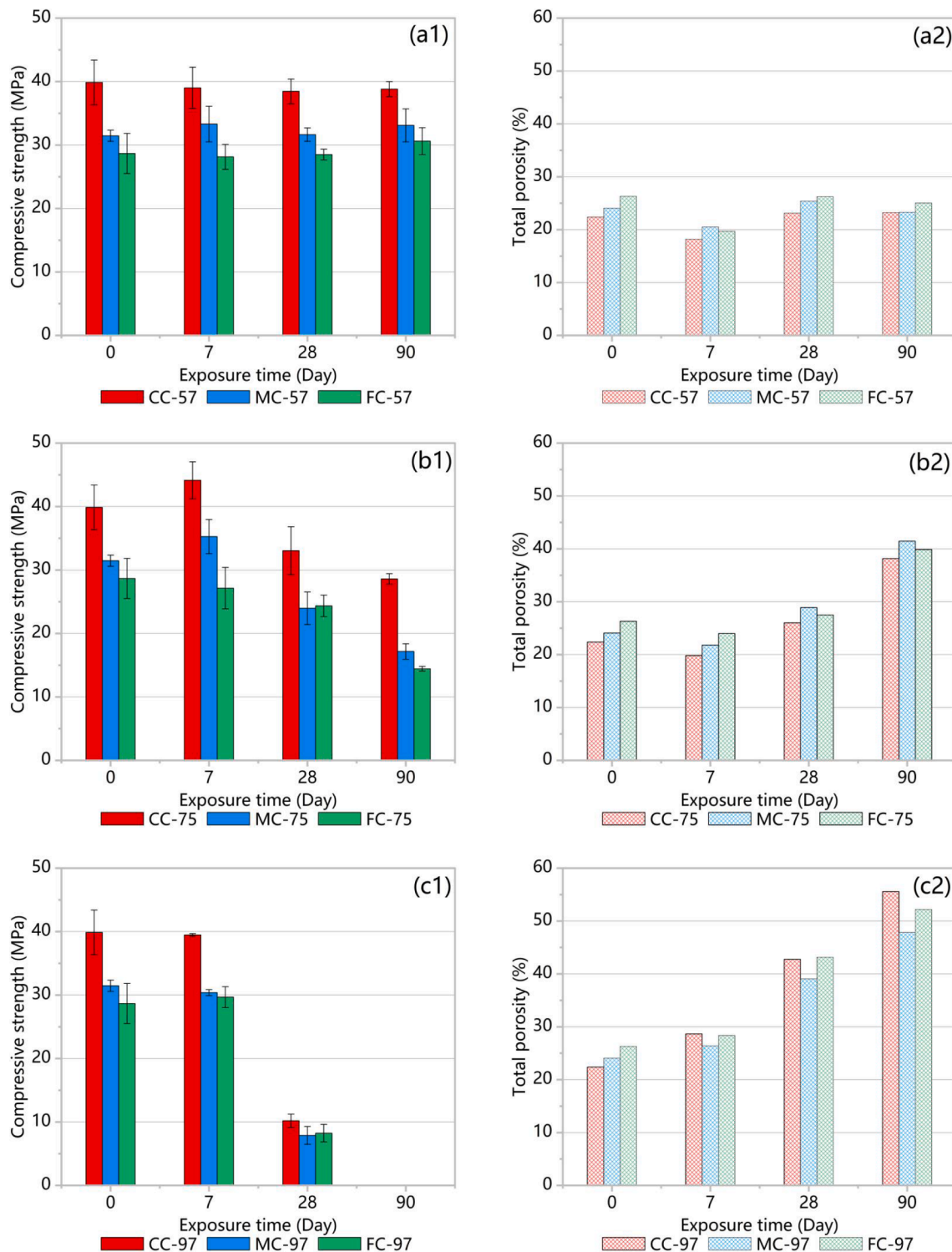


Fig. 10. Compressive strength (left) and Porosity (right) of anhydrous CSA cement and CSA cement with different PSD that pre-hydrated at 57% RH (a1,a2), 75% RH (b1,b2), 97% RH (c1,c2) for 0, 7, 28 and 90 days.

compared with fresh CSA cement (Fig. 11a), exposing CSA cement to 57% RH for 90 days (Fig. 11b) has less effect on the cumulative hydration heat of CSA cement. However, at higher exposure humidity (75% and 97% RH), the cumulative heat of hydration of CSA cement decreased steadily with the increase of exposure RH (Fig. 11c). This was caused by the reduced hydraulic activity of CSA cement, as portion of ye'elimitte and anhydrite in it was consumed by pre-hydration. Moreover, it was found that finer cement generally shows higher cumulative

heat during the first 10 h, and lower heat at the later stage of hydration (72 h). A similar trend has previously been reported [42]. No hydraulic activity was detected on CSA cement exposed to 97% RH for 90 days (Fig. 11d). The exothermic rate of cement hydration can be reflected by the heat flow. As can be seen from Fig. 11, FC sample (i.e., with finer cement powder) generally exhibits faster rate of hydration, followed by MC and CC sample. This is due to the lower median particle size and larger specific surface area of finer cement powder (FC sample)

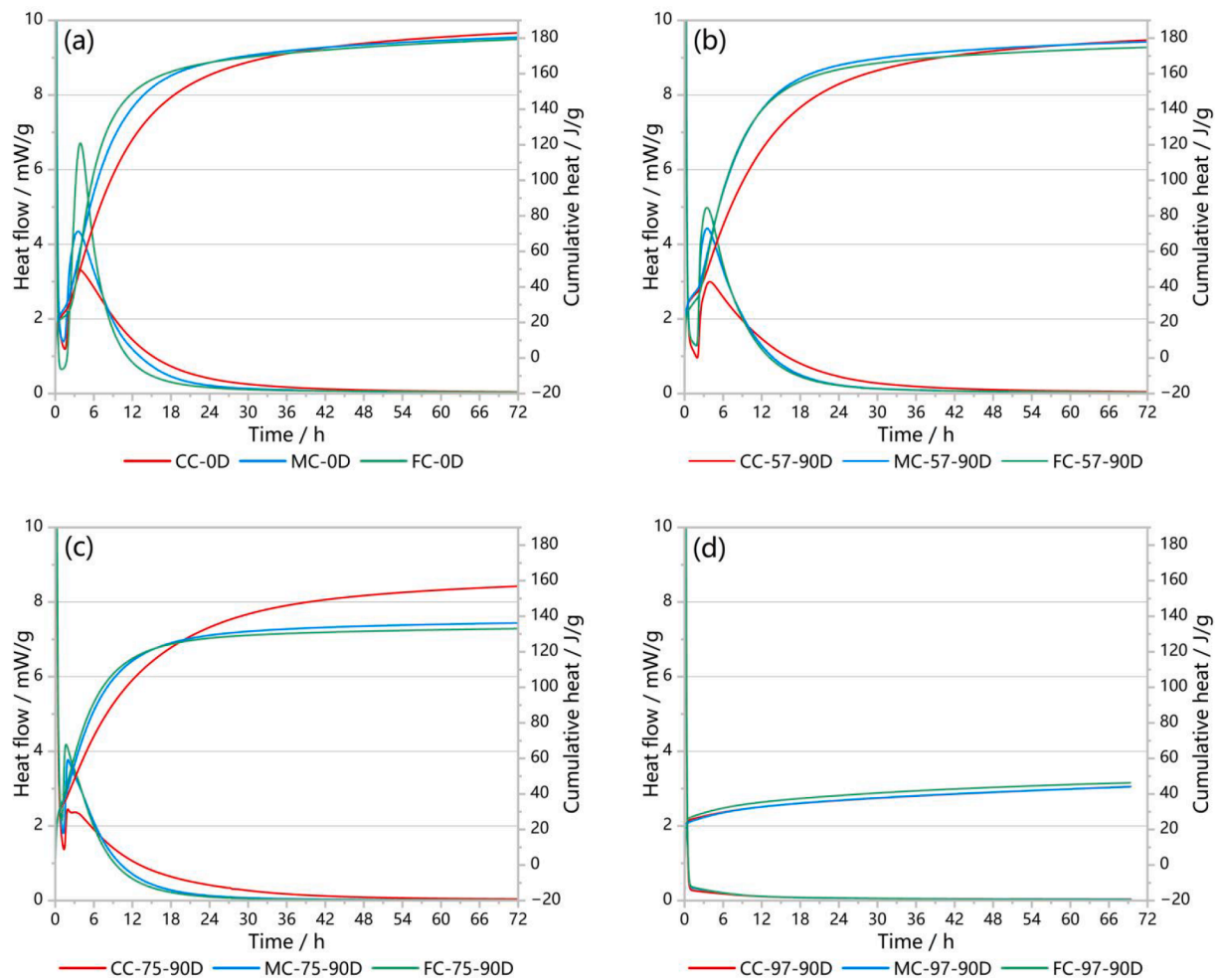


Fig. 11. Heat flow and accumulate heat of (a) anhydrous CSA cement and CSA cement with different PSD that pre-hydrated at (b) 57 %RH, (c) 75%, (d) 97 %RH for 90 days.

increased the overall contact area of cement powder with water therefore accelerates the dissolution rate of cement clinker at the early age. Similar results have been well documented in the literature [18,43,44].

Isothermal calorimetry results correspond well with compressive strength results (Fig. 10), where CC sample shown higher strength than MC and CC sample. The gentle exothermic peak and the higher cumulative heat of CC sample resulted in a higher degree of hydration and therefore higher compressive strength at 28 days.

4. Conclusions

In this study, the effect of PSD on the pre-hydration and further hydration behavior of CSA cement were experimentally studied. The amount of bound water, degree of pre-hydration, dynamic change of mineral assemblage of CSA cement which pre-hydrated at various exposure RH were quantified using CSA cement with three different PSD. After that, the coupled effect of PSD and pre-hydration on the hydration and compressive strength of CSA cement paste was studied from the perspective of hydration heat, compressive strength, and porosity. Based on the results reported above, the following conclusions can be drawn.

To guarantee a stable performance of CSA cement, the cement powder should be stored in an environment in which the RH is lower than 57%. The exposure of CSA cement to RH higher than that may result in pre-hydration of CSA cement. Ettringite and aluminum hydrates were found to be the main crystalline and XRD amorphous phase in the pre-hydration products, respectively. The degree of pre-hydration

of CSA cement increases with the elevation of exposure RH and the extension of exposure duration, which causes a reduction in the hydraulic activity of CSA cement and the compressive strength of hardened CSA cement paste. After exposed to 97 %RH for 90 days, no hydration heat and compressive strength could be measured on CSA cement.

The PSD of CSA cement has a significant impact on the pre-hydration, hydration kinetics and final properties of cement paste. Compared with the MC sample ($D_{50} = 10.8 \mu\text{m}$) and the FC sample ($D_{50} = 6.04 \mu\text{m}$), the CC sample with larger PSD ($D_{50} = 26.62 \mu\text{m}$) showed the best resistance to pre-hydration. It should be noted that the effect of PSD is not correlated linearly with the pre-hydration of CSA cement as fine particle of cement (FC sample) could have higher packing density of cement powder and delay the moisture from penetrating into the powder bed. However, with the increase of RH and the extension of exposure duration, the effect of pecking density becomes negligible.

CC sample with larger PSD showed not only higher resistance to pre-hydration, but also exhibited superior hardened stage properties such as compressive strength and porosity, irrespective of whether the CSA cement is freshly milled or exposed to moisture for a certain duration of time. The compressive strength of CC sample is at least 20% higher than MC and FC sample. Especially for CSA cement exposed to 75 %RH for 90 days, the compressive strength of CC sample is 28.6 MPa, which is 68.2% and 100% higher than MC and FC sample under the same exposure condition. This is further supported by the isothermal calorimetry measurements, where the relatively gentle exothermic peak and higher cumulative heat of CC sample contributes to the formation of cement paste with higher degree of hydration and lower porosity.

This study contributes to improving the performance of CSA cement, while lowering energy consumption and production costs in the manufacturing process. While not explored herein, further studies on the mitigation of pre-hydration and the optimization of PSD to achieve durable CSA cement products are important to further increase the potential for practical applications of CSA cement.

CRedit authorship contribution statement

Leyang Lv: Methodology, Supervision, Writing – review & editing. **Shitao Luo:** Investigation, Writing – original draft. **Branko Šavija:** Methodology, Writing – review & editing. **Hongzhi Zhang:** Supervision, Writing – review & editing. **Lin Li:** Writing – review & editing. **Tamon Ueda:** Writing – review & editing. **Feng Xing:** Writing – review & editing.

Declaration of Competing Interest

The authors declare that they have no known competing financial interests or personal relationships that could have appeared to influence the work reported in this paper.

Data availability

Data will be made available on request.

Acknowledgements

This work was supported by Guangdong Basic and Applied Basic Research Foundation (No. 2022A1515010765), Shenzhen Natural Science Foundation (No. 20220811031202001), Shenzhen Science and Technology Program (No. ZDSYS20220606100406016), Taishan Scholars Foundation of Shandong Province (No. tsqn201909032), 111 Project (No. B21012) and Natural Science Foundation of Jiangsu Province (No. BK20200235).

References

- [1] F. Preston, J. Lehne, Making concrete change innovation in low-carbon cement and concrete, chatham house -, The Royal Institute of International Affairs, 2018.
- [2] Energy Technology Perspectives 2017, IEA, Paris, 2017.
- [3] F. Winnefeld, B. Lothenbach, Hydration of calcium sulfoaluminate cements – Experimental findings and thermodynamic modelling, *Cem. Concr. Res.* 40 (8) (2010) 1239–1247.
- [4] M.C. Martín-Sedeño, A.J.M. Cuberos, Á.G. De la Torre, G. Álvarez-Pinazo, L. M. Ordóñez, M. Gatheski, M.A.G. Aranda, Aluminum-rich belite sulfoaluminate cements: clinkering and early age hydration, *Cem. Concr. Res.* 40 (3) (2010) 359–369.
- [5] F. Winnefeld, S. Barlag, Calorimetric and thermogravimetric study on the influence of calcium sulfate on the hydration of ye'elimite, *J. Therm. Anal. Calorim.* 101 (3) (2010) 949–957.
- [6] J. Pera, J. Ambrose, New applications of calcium sulfoaluminate cement, *Cem. Concr. Res.* 34 (4) (2004) 671–676.
- [7] S. Subramanian, Q. Khan, T. Ku, Strength development and prediction of calcium sulfoaluminate treated sand with optimized gypsum for replacing OPC in ground improvement, *Constr. Build. Mater.* 202 (2019) 308–318.
- [8] M.C.G. Juenger, F. Winnefeld, J.L. Provis, J.H. Ideker, Advances in alternative cementitious binders, *Cem. Concr. Res.* 41 (12) (2011) 1232–1243.
- [9] K. Quillin, Performance of belite-sulfoaluminate cements, *Cem. Concr. Res.* 31 (9) (2001) 1341–1349.
- [10] K. Ndiaye, M. Cyr, S. Ginestet, Durability and stability of an ettringite-based material for thermal energy storage at low temperature, *Cem. Concr. Res.* 99 (2017) 106–115.
- [11] B. Chen, K. Johannes, M. Horgnies, V. Morin, F. Kuznik, Characterization of an ettringite-based thermochemical energy storage material in an open-mode reactor, *J. Storage Mater.* 33 (2021), 102159.
- [12] B. Chen, K. Johannes, L. Ratel, M. Horgnies, V. Morin, F. Kuznik, Investigation on ettringite as a low-cost high-density thermochemical heat storage material: thermodynamics and kinetics, *Sol. Energy Mater. Sol. Cells* 221 (2021), 110877.
- [13] J. Stoian, T. Oey, J.W. Bullard, J. Huang, A. Kumar, M. Balonis, J. Terrill, N. Neithalath, G. Sant, New insights into the prehydration of cement and its mitigation, *Cem. Concr. Res.* 70 (2015) 94–103.
- [14] E. Dubina, L. Black, R. Sieber, J. Plank, Interaction of water vapour with anhydrous cement minerals, *Adv. Appl. Ceram.* 109 (5) (2013) 260–268.
- [15] O.M. Jensen, P.F. Hansen, E.E. Lachowski, F.P. Glasser, Clinker mineral hydration at reduced relative humidities, *Cem. Concr. Res.* 29 (9) (1999) 1505–1512.
- [16] L. Lv, B. Šavija, L. Li, H. Cui, N. Han, F. Xing, Prehydration of calcium sulfoaluminate (CSA) clinker at different relative humidities, *Cem. Concr. Res.* 144 (2021), 106423.
- [17] S. Ramanathan, B. Halee, P. Suraneni, Effect of calcium sulfoaluminate cement prehydration on hydration and strength gain of calcium sulfoaluminate cement-ordinary portland cement mixtures, *Cem. Concr. Compos.* 112 (2020), 103694.
- [18] D.P. Bentz, E.J. Garboczi, C.J. Haecker, O.M. Jensen, Effects of cement particle size distribution on performance properties of Portland cement-based materials, *Cem. Concr. Res.* 29 (10) (1999) 1663–1671.
- [19] Y. El Khessaimi, Y. El Hafiane, A. Smith, Effect of fineness and citric acid addition on the hydration of ye'elimite, *Constr. Build. Mater.* 258 (2020), 119686.
- [20] F. Sajedi, H.A. Razak, Effects of curing regimes and cement fineness on the compressive strength of ordinary Portland cement mortars, *Constr. Build. Mater.* 25 (4) (2011) 2036–2045.
- [21] V. Morin, P. Termkhajornkit, B. Huet, G. Pham, Impact of quantity of anhydrite, water to binder ratio, fineness on kinetics and phase assemblage of belite-ye'elimite-ferrite cement, *Cem. Concr. Res.* 99 (2017) 8–17.
- [22] R. Snellings, J. Chwast, Ö. Cizer, N. De Belie, Y. Dhandapani, P. Durdzinski, J. Elsen, J. Haufe, D. Hooton, C. Patapy, M. Santhanam, K. Scrivener, D. Snoeck, L. Steger, S. Tongbo, A. Vollpracht, F. Winnefeld, B. Lothenbach, RILEM TC-238 SCM recommendation on hydration stoppage by solvent exchange for the study of hydrate assemblages, *Mater. Struct.* 51 (6) (2018) 172.
- [23] Technology, Manufacturing, ASTM Designation No. E104-02 Standard Practice for Maintaining Constant Relative Humidity by Means of Aqueous Solutions, 02 (Reapproved 2012) (2012) 1-5.
- [24] L. Greenspan, Humidity fixed points of binary saturated aqueous solutions, *J. Res. Nat. Bureau Stand. Sec. A, Phys. Chem.* 81 (1) (1977) 89.
- [25] M. Zajac, J. Skocek, C. Stabler, F. Bullerjahn, M.B. Haha, Hydration and performance evolution of belite-ye'elimite-ferrite cement, *Adv. Cem. Res.* 31 (3) (2019) 124–137.
- [26] J. Zhang, G.W. Scherer, Comparison of methods for arresting hydration of cement, *Cem. Concr. Res.* 41 (10) (2011) 1024–1036.
- [27] K. Scrivener, R. Snellings, B. Lothenbach, A practical guide to microstructural analysis of cementitious materials, *Crc Press*, 2018.
- [28] G. Alvarez-Pinazo, A. Cuesta, M. García-Maté, I. Santacruz, E.R. Losilla, A.G.D. la Torre, L. León-Reina, M.A.G. Aranda, Rietveld quantitative phase analysis of Yeelimite-containing cements, *Cem. Concr. Res.* 42 (7) (2012) 960–971.
- [29] A. Cuesta, A.G. De la Torre, E.R. Losilla, V.K. Peterson, P. Rejmak, A. Ayuela, C. Frontera, M.A.G. Aranda, Structure, Atomistic Simulations, and Phase Transition of Stoichiometric Yeelimite, *Chem. Mater.* 25 (9) (2013) 1680–1687.
- [30] A. Kirfel, G. Will, Charge density in anhydrite, CaSO₄, from X-ray and neutron diffraction measurements, *Acta Crystallogr.* 36 (12) (1980) 2881–2890.
- [31] W.G. Mumme, R.J. Hill, E.R. Segnit, Rietveld crystal structure refinements, crystal chemistry and calculated powder diffraction data for the polymorphs of dicalcium silicate and related phases, *Neues Jahrbuch fuer Mineralogie - Abhandlungen* 169 (1) (1995) 35–68.
- [32] F. Goetz-Neunhoffer, J. Neubauer, Refined ettringite (Ca₆Al₂(SO₄)₃(OH)₁₂•26H₂O) structure for quantitative X-ray diffraction analysis, *Powder Diffr.* 21 (1) (2006) 4–11.
- [33] R. Allmann, Refinement of the hybrid layer structure hexahydroxaluminodicalcium hemisulfate trihydrate [Ca₂Al(OH)₆]+[(1/2 SO₄•3H₂O)], *Monatshfte, Neues Jahrbuch fur Mineralogie*, 1977, pp. 136–144.
- [34] T. Yamanaka, N. Hirai, Y. Komatsu, Structure change of Ca_{1-x}Sr_xTiO₃ perovskite with composition and pressure, *Am. Mineral.* 87 (8–9) (2002) 1183–1189.
- [35] S. Sasaki, K. Fujino, E. Tak, Y. Uchi, X-ray determination of electron-density distributions in oxides, mgo, mno, coo, and nio, and atomic scattering factors of their constituent atoms, *Proc. Japan Acad. Series B* 55 (2) (1979) 43–48.
- [36] C.W. Hargis, A.P. Kirchheim, P.J.M. Monteiro, E.M. Gartner, Early age hydration of calcium sulfoaluminate (synthetic ye'elimite, C4A3S) in the presence of gypsum and varying amounts of calcium hydroxide, *Cem. Concr. Res.* 48 (2013) 105–115.
- [37] Y. Zhao, X. Hu, C. Shi, Q. Yuan, D. Zhu, Determination of free chloride in seawater cement paste with low water-binder ratio, *Cem. Concr. Compos.* 124 (2021), 104217.
- [38] R.V. W., Effects of Storage on the Properties of Cement, *Zkg International* 2 (1973) 67–74.
- [39] M. Whittaker, E. Dubina, F. Al-Mutawa, L. Arkless, J. Plank, L. Black, The effect of prehydration on the engineering properties of CEM I Portland cement, *Adv. Cem. Res.* 25 (1) (2013) 12–20.
- [40] E. Dubina, R. Sieber, J. Plank, L. Black, Effects of pre-hydration on hydraulic properties on Portland cement and synthetic clinker phases, 28th cement and concrete science conference, Manchester, England, 2008.
- [41] F. Winnefeld, L.H.J. Martin, C.J. Müller, B. Lothenbach, Using gypsum to control hydration kinetics of CSA cements, *Constr. Build. Mater.* 155 (2017) 154–163.
- [42] J. Hu, Z. Ge, K.J. Wang, Influence of cement fineness and water-to-cement ratio on mortar early-age heat of hydration and set times, *Constr. Build. Mater.* 50 (2014) 657–663.
- [43] K. Van Breugel, Numerical simulation of hydration and microstructural development in hardening cement-based materials (I) theory, *Cem. Concr. Res.* 25 (2) (1995) 319–331.
- [44] M.P. Ginebra, F.C.M. Driessens, J.A. Planell, Effect of the particle size on the micro and nanostructural features of a calcium phosphate cement: a kinetic analysis, *Biomaterials* 25 (17) (2004) 3453–3462.